Astron. Astrophys. 324, 949–958 (1997)

ASTRONOMY AND ASTROPHYSICS

Properties of He-rich stars

I. Their evolutionary state and helium abundance⋆,⋆⋆

M. Zboril[1,⋆⋆⋆], **P. North**[2], **Yu.V. Glagolevskij**[3], **and F. Betrix**[2]

[1] Armagh Observatory, Armagh, College Hill, BT61 9DG, Northern Ireland
[2] Institut d'Astronomie de l'Université de Lausanne, CH-1290 Chavannes-des-Bois, Switzerland
[3] Special Astrophysical Observatory, Nizhnij Arkhyz, 357147 Russia

Received 6 January 1997 / Accepted 20 February 1997

Abstract. A determination of the surface gravity and an abundance analysis of helium in a sample of 17 He-rich and 5 normal, reference stars is presented. These results are derived from low resolution CCD spectra, but each star was measured at least 6 times in order to obtain a significant average spectrum for the spectroscopic variables. The helium abundances derived from the models used are very close to 0.1 for normal, reference stars and are larger for the others, clearly indicating the He-rich phenomenon in them. NLTE effects, errors on the microturbulence value or on the surface gravity do not influence the estimated helium abundances. Nevertheless, synthesized Geneva colours are affected by the He-rich peculiarity, especially the [U-B] index which systematically changes by -0.025 mag per 0.1 of He abundance for the coolest stars in the sample.

We cannot confirm the correlation between the evolutionary state and the helium abundance reported previously (Zboril et al. 1994), although we used a more reliable technique of $\log g$ determination. All He-rich objects lie within the main sequence: their surface gravities are all inside the range $4.1 < \log g < 4.5$, with no more than three objects having $\log g < 4.25$. We find a significant spread of helium abundances in this range of surface gravities, from the solar value ~ 0.1 up to about 0.4. Some of the programme stars (including reference stars) present emission in their Balmer lines and therefore some kind of stellar activity. Strong helium overabundance often coexists with emission and stellar activity.

Key words: stars: abundances – stars: atmospheres – stars: chemically peculiar – stars: fundamental parameters

Send offprint requests to: M. Zboril

⋆ Based on observations collected at the European Southern Observatory, La Silla, Chile

⋆⋆ Table 1 is only available in electronic form at the CDS via anonymous ftp to cdsarc.u-strasbg.fr (130.79.128.5) or via http://cdsweb.u-strasbg.fr/Abstract.html

⋆⋆⋆ On leave from Astronomical Institute, 05960,Tatranská Lomnica, Slovakia

1. Introduction

He-rich stars are the most massive chemically peculiar (CP) stars: their spectral type is around B2, and they belong to the main sequence. Their helium lines are anomalously strong for their colours, implying abundances $n(\mathrm{He})/n(\mathrm{H}) \sim 0.5$ in their atmosphere, instead of ~ 0.1. Most of them are magnetic, like the cooler Ap Si and SrCrEu stars, but with fields about 3 times stronger (Bohlender et al. 1987). They also show spectral, light and magnetic variability, like the other magnetic CP stars (Pedersen & Thomsen 1977, Pedersen 1979). They are generally considered as belonging to the same family as the magnetic Ap stars, because of the many characteristics they share with them. Their abundance anomalies are interpreted as due to a diffusion mechanism involving a competition between the radiative and gravitational forces in the atmosphere, in the presence of a wind (Vauclair 1975; Michaud et al. 1987; Vauclair et al. 1991). Vauclair (1975) was the first to show that a wind is required to accumulate helium in the atmosphere because otherwise this element would sink. Michaud et al. (1987) mention that their model predicts normal abundances of the CNO elements, which indeed agrees with the observations, as a forthcoming paper will confirm.

The main review of the observational properties of He-rich stars remains the work of Walborn (1983). He has observed 19 such stars, taking photographic spectrograms at 39 Åmm^{-1}. He published equivalent widths of hydrogen, helium and metallic lines as well as projected rotational velocities, which appear to be similar to those of normal B stars. He also discussed the evolutionary state of these stars, but faced a problem with the scale of his equivalent widths.

Since the work of Walborn, there has been as yet no systematic survey of the spectroscopic properties of these stars using a linear detector. To fill this gap, and to tighten the constraints on the theoretical models of He-rich stars, we have observed a sample at both low and high dispersion with CCD detectors. This paper is the first of a series and describes the abundance analysis of helium for 17 He-rich stars and 5 normal reference

stars. We give the helium abundance and its dependence upon the surface gravity, interpreted as an age indicator on the main sequence. The main purpose of this paper is indeed to confirm the correlation between the He abundance and surface gravity found by Glagolevskij et al. (1992) and by Zboril et al. (1994) on smaller samples.

2. Observations and reduction

One of us (PN) obtained a total of 155 spectra for 24 stars in the spectral range 395.2 – 493.8 nm using the 1.5m spectrographic telescope and the Boller & Chivens spectrograph at the European Southern Observatory, La Silla, Chile. The grating used was #20 (ESO numerotation) in the second order; it has a blaze wavelength of 455 nm and 1200 grooves per millimeter, giving a reciprocal dispersion of 32 Åmm^{-1}, a resolution of 1.08 Å (about 2 pixels per Å) and a resolving power R = 4150. The width of the entrance slit was 329 μm, i.e. 3". The detector was ESO CCD #24, a Ford Aerospace 2048 $\times$ 2048 chip with 15 $\times$ 15μm pixels. The integration times varied typically between 3 and 20 minutes according to the star's brightness.

The journal of the observations is given in Table 1. Six out of the 24 stars observed are defined as $v \sin i$ standards by Slettebak et al. (1975). One different standard star was observed each night, while each He-rich star was observed in several nights, typically in 3 to 6 nights. The raw data were reduced by FB using the TACOS software developed at Geneva Observatory. The procedure was the same as that used by North & Paltani (1994) and implied an extraction of the spectrum using the Horne algorithm. The wavelength calibration was done using He-Ar exposures done at the beginning and at the end of each night. Since we were not interested in precise radial velocities, we did not make a He-Ar exposure after each observation. Therefore our wavelength scale may be slightly in error, in a different way for each star, because of instrumental flexures. But this cannot affect our present analysis in a significant way. After wavelength rebinning, we defined a continuum interactively, and the points chosen were linked by a third-degree spline function. The spectra were then divided by this continuum.

3. Analysis

The following transitions were identified and used in the spectra. Concerning neutral helium, we analysed the transitions 396.4, 400.9, 402.6, 412.0, 414.3, 438.7, 443.7, 447.1, 471.3 and 492.1 nm. The transitions 402.3 and 416.8 nm are also visible but considerably weaker. The transitions of primary interest are 402.6, 414.3, 438.7 and 492.1 nm: their equivalent widths are given in Table 2, allowing a comparison with Walborn's data (Fig. 1). Other helium transitions were either in hydrogen wings and blended (396.4, 412.0 nm) or blended (447.1 and 471.3 nm). In the case of some (hot) stars transitions belonging to singly ionized helium were also identified: 410.0, 419.9, 433.8, 454.1, 468.5 and 489.5 nm.

Since we primarily concentrated on helium abundance and its age dependence, we cross-correlated and co-added the spectra from individual nights to increase the S/N ratio at least in cases of nonvariables by using the code Corel (written by MZ) for numerical correlation. Subsequently, the equivalent widths were measured by numerical integration; the results are given in Table 2. The star HD 68450 has been removed eventually, since it is clearly a very special case: it has been classified O9.7 Ib-II (e.g. Prinja et al. 1990). Indeed, hydrogen line profiles are extremely narrow and have a peculiar shape in this object. This probably explains the 0.3 dex difference in helium abundance found using high resolution CCD spectra in a previous study (Zboril et al. 1994). Likewise, the star HD 124448 (Popper's star) is not a member of the "intermediate" helium stars (as the He-rich stars considered here are sometimes called), but is extremely hydrogen-poor and is probably a post-AGB star evolving towards the white dwarf state (Schönberner & Wolf 1974).

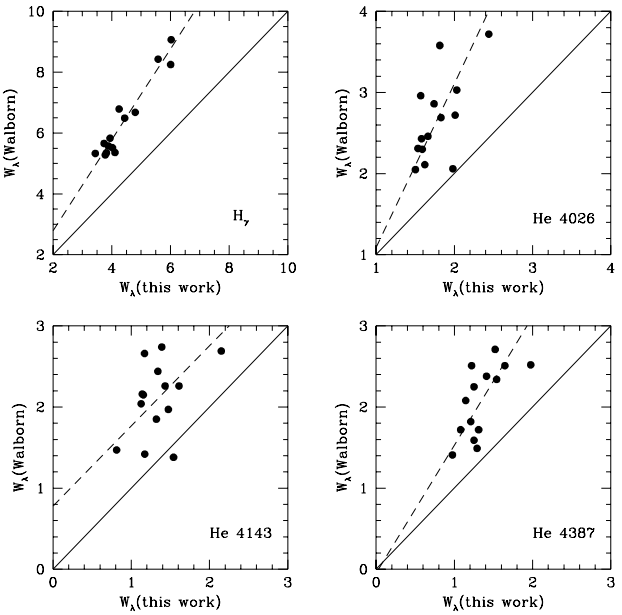

Fig. 1. Comparison between Walborn's equivalent widths and ours for Hγ and three He I lines.The full lines represent the equality, while the broken lines are the regression ones, assuming that our values are three times more precise than Walborn's.

3.1. Atmospheric parameters and modeling the atmospheres

To derive the atmospheric parameters of our stars we used the following criteria: H$_\beta$ and H$_\gamma$ equivalent widths and Glagolevskij's (1990) calibration, Geneva photometry calibrated by Kűnzli et al. (1997), and theoretical H$_\beta$, H$_\gamma$ and H$_\delta$ profiles using Kurucz's (1992) model atmospheres. Final estimates are given in table 4. They were obtained using the following order of priority among the criteria adopted, namely: (1) Balmer line profiles, (2) Balmer line equivalent widths and Glagolevskij's (1990) calibration, (3) Geneva photometry. The last 5 stars in Table 4 are reference ones. Since UBV and Strőmgren measurements are available only for less than half of the stars, we used as a photometric method the Geneva photometry which is available for all programme stars but CpD

Table 2. Hγ and helium λ402.6Å, 414.3, 438.7 and 492.2 nm equivalent widths in Å.

Star	Hγ	402.6	414.3	438.7	492.2
36485	6.010	1.580	1.340	1.250	0.880
37017	5.580	1.570	1.170	1.220	0.902
37479	3.440	2.010	1.473	1.645	1.172
37776	3.740	1.830	1.432	1.520	1.202
260858	4.440	1.740	1.154	1.145	0.994
264111	3.945	1.980	1.540	1.310	1.125
-27	4.801	1.590	1.140	1.080	0.921
58260	3.890	1.813	1.390	1.411	1.092
60344	4.110	1.662	1.320	1.250	0.950
64740	4.022	1.622	1.172	1.290	1.105
66522	4.250	2.030	1.610	1.540	1.264
-46	3.820	1.535	1.126	1.210	1.118
92938	6.960	1.175	0.685	0.730	0.575
96446	3.780	2.440	2.150	1.975	1.540
-62	2.702	2.204	1.865	1.940	1.334
108483	5.122	1.481	0.952	0.946	0.866
124448	—	2.820	2.115	2.302	1.984
133518	4.825	1.863	1.290	1.294	1.073
56139	3.970	1.128	0.674	0.626	0.604
105435	2.602	1.040	0.672	0.548	0.340
110879	6.025	1.503	0.812	0.975	0.754
121790	4.960	1.470	0.910	0.932	0.808
122980	5.530	1.540	0.930	0.940	0.842

$-62°2124$. Also since the spectral region covered is wide (about 1000 Å), we could use three hydrogen lines to derive the atmospheric parameters from LTE Kurucz models: we modeled Hβ, Hγ and Hδ and fitted them to coadded observed profiles by means of a least-squares method. The Hγ line proved very suitable since the corresponding χ^2 sum remained small for all spectral types. In this way, we got 6 estimates of effective temperature and surface gravity for each star because two best estimates were considered for every hydrogen profile. As a first step, data from photometry were considered only as a complementary method in some special cases. Even though emission was detected in the observed hydrogen profiles in a few stars, only in the case of HD 56139 (a normal, comparison star) were the photometric and spectroscopic effective temperatures different by as much as $\sim$ 7000 K; the spectroscopic method overestimates the temperature because it underestimates the intensity of the H_β line, which is partly filled with emission, while Strömgren's c_0 parameter or Geneva's X parameter is free from it. Fig. 2 illustrates the fit in the case of HD 92938.

The following relations were found between three criteria for T_{eff}:

$$T_{Glagol} = 0.874 \times T_{spectro} + 2790 \quad (1)$$

$$T_{Geneva} = 0.978 \times T_{spectro} + 1308 \quad (2)$$

$$T_{Geneva} = 1.118 \times T_{Glagol} - 1750 \quad (3)$$

with rms standard deviations of the residuals of 1194, 1021 and 871 K respectively, and where $T_{spectro}$ is the effective temperature derived from the observed and synthetic Balmer line profiles. These relations where obtained with the macro *lsq2* of the *supermongo* package, which allows for errors not only on the y axis, but also on the x axis (here we assumed similar errors on both axes). Thus, estimates from Geneva photometry are closest to the values derived from the profiles of the hydrogen lines, in the sense that the slope is almost unity and the scatter of the residuals is minimum. However, there is a systematic shift of 1300 K, the photometry giving higher temperatures than spectroscopy. This systematic difference is difficult to explain, but it might be due to the non-standard helium abundance. Unfortunately, we do not have spectra of the normal, standard stars used by Künzli et al. (1997) to calibrate the Geneva system in $T_{\rm eff}$.

Table 3. LTE and NLTE Geneva colours for log g = 4.0 models.

colour index	Effective temperature					
	16000		20000		25000	
	LTE	NLTE	LTE	NLTE	LTE	NLTE
n(He) = 0.1:						
U-B	0.613	0.605	0.384	0.377	0.216	0.215
B-V	-1.122	-1.124	-1.170	-1.171	-1.226	-1.227
V-B1	0.322	0.324	0.389	0.391	0.464	0.465
B1-B2	-0.792	-0.793	-0.835	-0.837	-0.877	-0.877
B2-V1	-0.225	-0.226	-0.248	-0.248	-0.279	-0.279
V1-G	-0.524	-0.525	-0.533	-0.533	-0.545	-0.545
n(He) = 0.4:						
U-B	0.514	0.486	0.309	0.294	0.176	0.165
B-V	-1.106	-1.100	-1.149	-1.152	-1.212	-1.214
V-B1	0.307	0.313	0.371	0.374	0.451	0.453
B1-B2	-0.794	-0.800	-0.838	-0.841	-0.878	-0.880
B2-V1	-0.208	-0.209	-0.228	-0.228	-0.265	-0.266
V1-G	-0.521	-0.521	-0.526	-0.526	-0.540	-0.539

Strangely enough, the surface gravities derived from Geneva photometry are not well correlated with those derived in a purely spectroscopic way from the Balmer line profiles (see open dots in Fig. 4). Hydrogen line profiles are sensitive to both effective temperature and surface gravity. On the other hand, the Balmer jump measured by Geneva photometry is essentially sensitive to temperature, but is also affected by helium abundance. Therefore we have estimated the effect of the helium abundance on the Geneva colours (see next subsection) and redetermined the surface gravities from the Balmer line profiles, but using this time the effective temperatures from Geneva photometry (effect of He abundance included) as a fixed parameter. We then obtain a slightly better agreement between the spectroscopic and photometric estimates of the surface gravity (black dots in Fig. 4). Here again, all log g values are larger than 4.0, as in the photometric estimates.

3.2. Revised photometric $T_{\rm eff}$ and hydrogen profile

The Balmer jump may be affected by the enhanced helium abundance, due to both $b-f$ and $b-b$ transitions of helium. This fact was established using fully consistent model atmospheres. Having taken passbands functions from Rufener & Nicolet (1988), we computed theoretical Geneva colours which are presented in Table 3, by integrating the flux at the stellar surface. Models

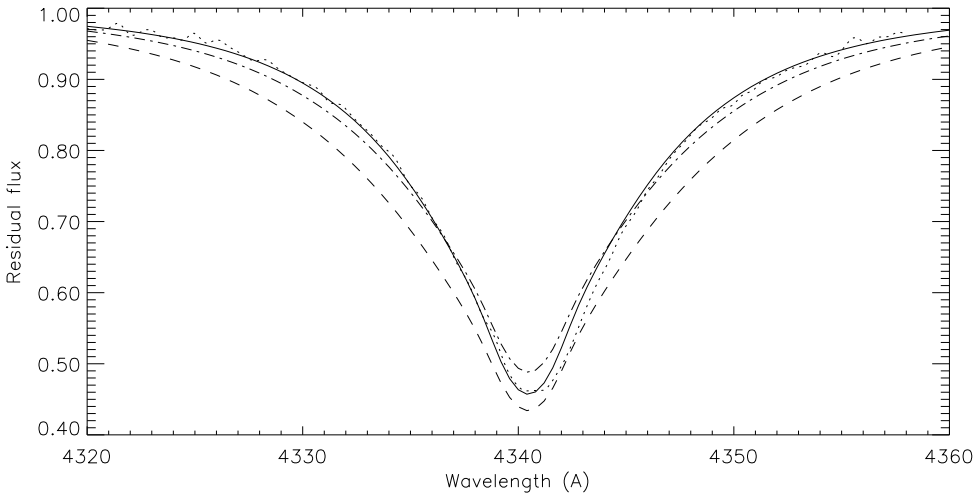

Fig. 2. H_γ profile for HD 92938. **Dots:** coadded spectra from 7 nights, **solid line:** synthesized line profile from Kurucz (1992) models with T_{eff} = 15000K, $log\ g$ = 4.0, **dashed dotted line:** T_{eff} = 17000K, $log\ g$ = 4.5, **dashed line:** T_{eff} = 15000K, $log\ g$ = 4.5. Synthetic profiles were convolved with $vsini$ = 130 kms^{-1} and a gaussian with FWHM = 1 Å.

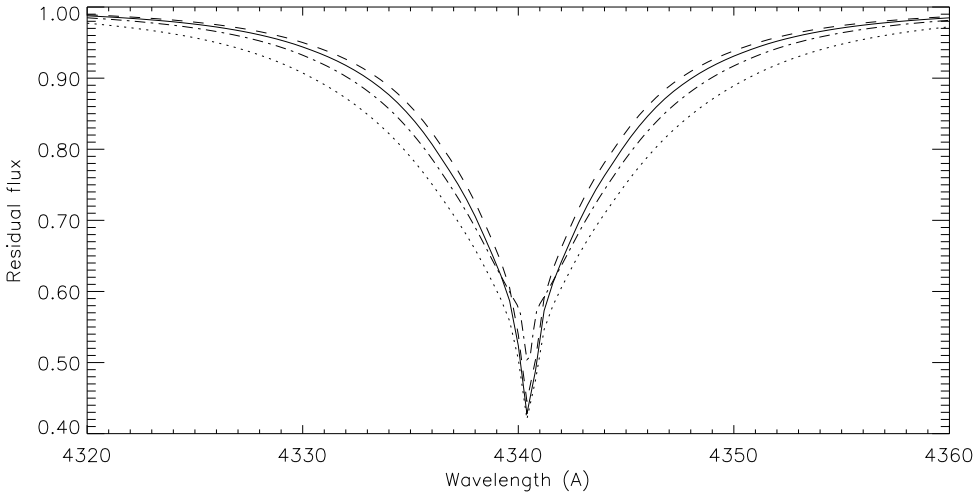

Fig. 3. A part of H_γ profile from Kurucz models (1992). **Dots:** T_{eff} = 19000K, $log\ g$ = 4.5, **solid line:** 19000K, 4.0, **dashed dotted line:** 19000K, 4.5, NLTE option+$n(He)$ = 0.25, **dashed line:** 20000K, 4.0. Other models have solar abundances. No rotational broadening.

have been computed with log g = 4.0 and $T_{\rm eff}$ = 16000, 20000 and 25000 K, in the LTE and NLTE approximations an for the two helium abundances n(He)=0.1 and 0.4 (n(H)=1.0). Table 3 allows to intercompare the effect of the overabundance of He on the Geneva colours.

According to the table, the $[U-B]$ index of the Geneva photometric system is most affected by the He-rich peculiarity. Other Geneva indices change by only a few mmag, which remains within the standard measurements' scatter. Therefore, the He-rich peculiarity affects essentially the $T_{\rm eff}$ estimate, while the estimate of the surface gravity (essentially measured by the $B1-B2$ index which is included in the reddening-free Y parameter) remains unaffected in practice.

Geneva colours were revised according to the above table applying two-dimensional (He abundance, $T_{\rm eff}$) fits; this means they were corrected to a standard helium abundance $n(He)$ = 0.1 so that they yield meaningful, unbiased $T_{\rm eff}$ estimates. Test runs indicate a much higher dependence of the fluxes to non-solar abundances of helium and other elements than to pure NLTE effect.

We can also see from Fig. 3 that if hydrogen profiles are processed with solar helium abundance we may get inconsistency. Therefore we processed profiles with expected abundances obtained with the LTE approximation and computed NLTE line profiles. The NLTE option plays a role in line cores, as expected since it depends directly on level populations. The deeper into the atmosphere, the closer the NLTE departure coefficient is to unity. Helium abundance therefore should play a role in line wings. Hydrogen profiles were processed using the standard VCS broadening theory. It is worth noting that in the temperature interval of the programme stars the hydrogen profiles are much more sensitive to surface gravity. We may also expect better agreement with temperature from Geneva photometry. In addition, this hydrogen profile effect maintains over the whole temperature range $\sim$ 16000-25000K in which most of our programme stars lie.

Finally, we quote in Table 4 the atmospheric parameters obtained with both methods, except for HD 56139 and HD 105435 where values from photometry were preferred: the spectroscopic parameters would imply that these stars are strongly He-weak, while emission is clearly present.

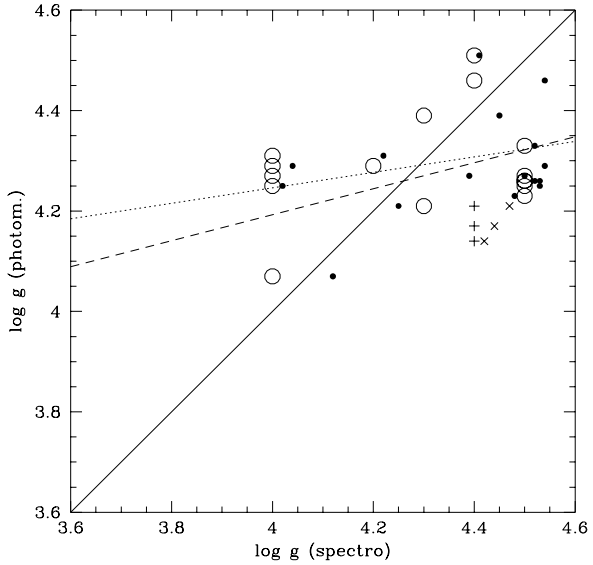

Fig. 4. Photometric versus spectroscopic surface gravities for the programme stars. **Open symbols:** Purely spectroscopic values for the He-rich stars, T_{eff} being also determined from the Balmer line profiles; + symbols are for normal stars. **filled symbols:** Spectroscopic values obtained assuming the photometric T_{eff} corrected for the effect of He abundance (He-rich stars); x symbols are for normal stars. The continuous line is the equality. The broken line is a regression line fitted through the black dots, while the dotted line has been fitted through the open dots.

For the microturbulence, we adopted here the depth-independent value v_{turb} = 6 $km\,s^{-1}$, an average of Kilian's (1992) determinations for early type stars. Although Kilian (1992) found a loose correlation between v_{turb} and $\log g$, we adopted here a constant value. Most helium lines lie on the third part of the curve-of-growth and microturbulence should not be significant in this case; indeed, due to the large values of equivalent widths, the influence of microturbulence is not crucial. A set of helium abundances for two values of microturbulence is computed in each case. The investigation of microturbulent values and their behaviour together with the abundance of CNO and other elements as well as rotational velocities ($v \sin i$) will be presented in another paper.

Once the atmospheric parameters were derived we proceeded with model atmosphere computations in two ways: first, we adopted Kurucz (1992) LTE model atmospheres and computed detailed helium line profiles and equivalent widths. Thus, the model atmosphere was not actually computed. Second, since the He-rich stars are early type stars we computed several consistent NLTE model atmospheres following LTEGray-LTE-NLTEC-NLTEL sequence. The LTEGray abbreviation stands for initial LTE-gray model atmosphere while NLTEC is for NLTE model for continua and NLTEL for NLTE model for lines, i.e. bound-bound transitions.We used the NLTE code Tlusty (Hubeny and Lanz 1992) from the CCP7 library to make these computations. Once an LTE model was computed, we computed in a subsequent run a NLTE model to check the NLTE level populations for helium and their possible consequence on the equivalent widths as well as NLTE model atmosphere for the computation of hydrogene line profiles. The criterion of convergence was that the maximal relative change of any physical quantity in the model (temperature, total particle number, electron density) and level populations do not exceed 0.001 at each depth point.

We performed fully consistent computations, starting with solar composition atmosphere models and modifying iteratively the He abundance until the synthetic He profiles agreed with the observed ones. Besides typical continuous opacities valid for B-A type stars (H−, H_2^+, Rayleigh scattering) we considered 42 explicit levels: 5 levels of neutral hydrogen, 1 level of ionized hydrogen, 30 levels of neutral helium (the states: 1 sing S, 2 trip S, 2 sing S, 2 trip P, 2 sing P, 3 trip S, 3 sing S, 3 trip P, 3 trip D, 3 sing D, 3 sing P, 4 trip S, 4 sing S, 4 trip P, 4 trip D, 4 sing D, 4 trip F, 4 sing F, 4 sing P, 5 trip S, 5 sing S, 5 trip P, 5 trip D, 5 sing D, 5 sing F, 5 trip F, 5 sing P, $< n = 6 >$, $< n = 7 >$, $< n = 8 >$), 1 level of ionized helium, 2 levels of neutral carbon (the states: 2 sing S, 2 sing D), 2 levels of singly ionized carbon (2 dubl $P_{1/2}$, 2 dubl $P_{3/2}$) and 1 level of doubly ionized carbon which contributes to the continuum opacity due to bound-free transitions (abbrevation <> denotes averaged levels with principal quantum number but not mixing singlet and triplet states). The transitions 396.4, 402.6, 438.7, 447.1, 471.3 and 492.1 nm for He were processed as explicit transitions: radiative rates are linearized, the other helium transitions were considered in detailed radiative balance, radiative rates are not evaluated but collisional rates are. Explicit energy levels chosen cover the observed He I neutral lines satisfactorily. Here we stress that the attention is paid to investigations of potential impact of NLTE on helium abundances and evolutionary state since NLTE level populations are both abundance and temperature dependent. The procedure above was not successful for very He-rich stars, i.e. with helium abundance roughly 0.25 and more, due to problems with the convergence of the models. Some test runs indicate that even not converging models (maximal relative change of order 0.1-0.01) might be applicable, but if they are not fully physically consistent, they are not reported here.

3.3. Helium abundances

Helium abundances were computed using Hubený's code Synspec modified by Zboril (1996). Helium line profiles were computed in the following way:

447.1 nm after Barnard, Cooper and Smith (1974), 402.6, 438.7 and 492.2 nm after Shamey (1969) and the other neutral helium lines after Dimitrijevic and Sahal-Brechot (1984). Singly ionized helium lines were computed after Schoening and Butler (1989). An example of co-added spectra and comparison with synthesized ones is given in Figs. 5 and 6. Synthetic spectra were computed with solar composition for all elements except for helium.

Once the model atmosphere was chosen (Kurucz LTE model) and the helium line profiles and equivalent widths com-

Table 4. Atmospheric parameters and evolutionary state for He-r stars obtained using Kurucz models. The quantities with the "*new*" superscript have been obtained assuming the corrected photometric $T_{\rm eff}$, while the others have been obtained from the Balmer line profiles alone.

Star	$T_{\rm eff}$	log g	$T_{\rm eff}^{new}$	log g^{new}	R/R_z	He abundance	R/R_z^{new}	He^{new}	emis.
36485	18000	4.4 ± 0.11	18400	4.41 ± 0.11	0.85 ± 0.11	0.14 ± 0.07	0.84 ± 0.11	0.15	
37017	18500	4.3 ± 0.10	19200	4.45 ± 0.10	0.95 ± 0.11	0.14 ± 0.08	0.80 ± 0.09	0.12	
37479	22000	4.5 ± 0.17	22200	4.53 ± 0.17	0.76 ± 0.15	0.22 ± 0.09	0.73 ± 0.11	0.32	e
37776	22000	4.5 ± 0.07	21800	4.52 ± 0.07	0.76 ± 0.06	0.19 ± 0.09	0.74 ± 0.06	0.22	
260858	18000	4.0 ± 0.10	19200	4.22 ± 0.10	1.35 ± 0.16	0.24 ± 0.10	1.05 ± 0.12	0.19	
264111	22400	4.2 ± 0.06	23200	4.54 ± 0.06	0.85 ± 0.06	0.20 ± 0.11	0.72 ± 0.06	0.30	
$-27°3748$	23000	4.5 ± 0.11	22700	4.53 ± 0.11	0.76 ± 0.10	0.13 ± 0.06	0.73 ± 0.09	0.18	
58260	19000	4.0 ± 0.19	19000	4.02 ± 0.18	1.35 ± 0.29	0.27 ± 0.10	1.32 ± 0.22	0.21	e
60344	21000	4.5 ± 0.18	21700	4.48 ± 0.18	0.76 ± 0.16	0.16 ± 0.10	0.78 ± 0.15	0.21	
64740	21000	4.5 ± 0.06	22700	4.50 ± 0.06	0.76 ± 0.05	0.13 ± 0.08	0.76 ± 0.06	0.18	
66522	18000	4.0 ± 0.10	18800	4.39 ± 0.10	1.35 ± 0.16	0.38 ± 0.12	0.86 ± 0.10	0.32	
68450	32500	4.0	32300	4.05	–	–	1.27	–	e
$-46°4639$	22500	4.5 ± 0.11	22000	4.52 ± 0.11	0.76 ± 0.11	0.13 ± 0.08	0.74 ± 0.09	0.22	
92938	15000	4.0 ± 0.10	15000	4.12 ± 0.10	1.35 ± 0.16	0.20 ± 0.08	1.17 ± 0.13	0.20	
96446	20500	4.4 ± 0.21	22000	4.54 ± 0.20	0.85 ± 0.21	0.38 ± 0.12	0.72 ± 0.17	0.37	e
$-62°2124$	26000	4.2 ± 0.21	–	4.23 ± 0.20	1.07 ± 0.26	$\sim 0.81 \pm 0.15$	1.04 ± 0.23	–	e(H)
108483	19200	4.3 ± 0.10	19100	4.25 ± 0.10	0.76 ± 0.09	0.12 ± 0.05	1.01 ± 0.12	0.11	
124448	–	–	22000	3.7	1.91 ± 0.46	<0.8 ?	–	<0.8	e(H)
133518	17500	4.0 ± 0.10	18600	4.04 ± 0.10	1.35 ± 0.16	0.29 ± 0.10	1.29 ± 0.14	0.23	
56139	–	–	18000	3.63 ± 0.18	–	–	1.93 ± 0.38	0.12 ± 0.05	e(H)
105435	–	–	26000	4.51 ± 0.20	–	–	0.75 ± 0.17	0.08 ± 0.05	e(H)
110879	18000	4.4 ± 0.07	18200	4.47 ± 0.07	0.76 ± 0.06	0.10 ± 0.05	0.79 ± 0.06	0.11	
121790	19500	4.4 ± 0.11	19600	4.42 ± 0.11	0.76 ± 0.10	0.10 ± 0.06	0.83 ± 0.11	0.12	
122980	18500	4.4 ± 0.10	19600	4.44 ± 0.10	0.76 ± 0.09	0.11 ± 0.06	0.81 ± 0.09	0.12	

puted, the evolutionary state of each star was defined by the ratio R/R_z which was computed according to the equation

$$log(R/R_{ZAMS}) = \frac{1}{2}(log\ g_{ZAMS} - log\ g) \quad (4)$$

Using Tables 8 to 10 of Schaller et al. (1992), and applying the transformation

$$log\ g = -10.607 + log(M/M_\odot) + 4logT_{eff} - log(L/L_\odot) \quad (5)$$

one obtains $log\ g_{ZAMS}$ = 4.291,4.265, 4.262, 4.251 and 4.234 for M = 5, 7, 9, 12 and 15 $M_\odot$ respectively. Since $log\ g_{ZAMS}$ is nearly independant of the mass, we adopt here the constant value 4.26 when applying Eq. 4.

The evolutionary state is presented in Table 4; in this table are also listed the helium abundances obtained, and the errors indicated represent in fact the rms scatter from the different transitions used. The errors on R/R$_z$ are evaluated adopting the usual expression for propagation of errors, giving:

$$\sigma(\frac{R}{R_z}) = \frac{ln10}{2}\frac{R}{R_z}\sigma(log\ g) = 1.15\frac{R}{R_z}\sigma(log\ g) \quad (6)$$

where σ(log g) is the error on surface gravity. The same goes for helium abundance where we consider as three main error sources: equivalent width measureuments (typically 4-5 percents), T_{eff} and log g estimates. In Table 4, the symbol new stands for new estimates using the corrected photometric $T_{\rm eff}$ in the spectroscopic estimation of log g, as explained above. HD 68450, which is very hot, and HD 124448 are both clearly atypical (as explained in Sect. 3) but are nevertheless listed, although they will not be considered in the final analysis. An 'e' symbol denotes emission, while the '(H)' symbol means that the emission is clearly present in the H$_\gamma$ profile; the 'e' symbol alone means that emission in H$_\beta$ is recognized from a comparison between the observed β index of $uvby\beta$ photometry and the β_c parameter computed from Geneva photometry according to Cramer & Maeder (1979). The solar value adopted is 0.1 relative to hydrogen (n(H)=1.0).

3.4. NLTE helium level populations

Generally, departure from local thermodynamic equilibrium is easily seen in hot stars since many quantitites (Saha-Boltzmann relation, radiative and collisional rates etc.) depend upon temperature and partly on the intensity of the radiative field. However, a NLTE situation is also present in cool stars and the Sun in their upper atmosphere, because of an anomalous temperature behaviour associated with population and depopulation processes. As mentioned already, He-rich stars occupy a wide interval of temperatures and have non-solar helium abundances, so we decided to check the helium abundances considering the NLTE option of the Tlusty and Synspec programmes. In the case of bound-free helium transitions, we used relations after Opacity Project (up to level 4); otherwise, we used the hydrogenic approximation with exact Gaunt factors. Collisional rates (excitation and ionization) were calculated following the special procedure by Hummer, which is already included in the programme, and following Mihalas et al. (1975).

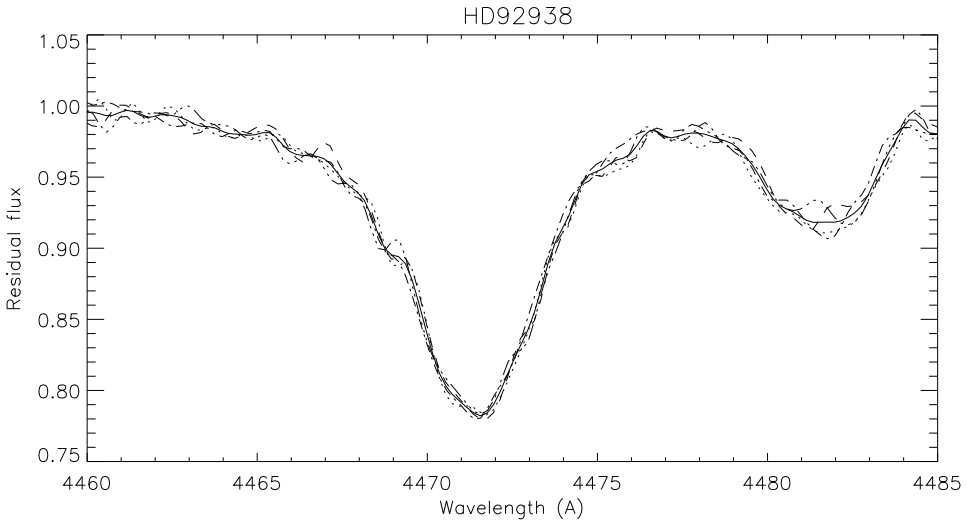

Fig. 5. He I λ 4471 Å line profile of HD 92938 from 4 nights, and corresponding coadded spectrum (**solid** line).

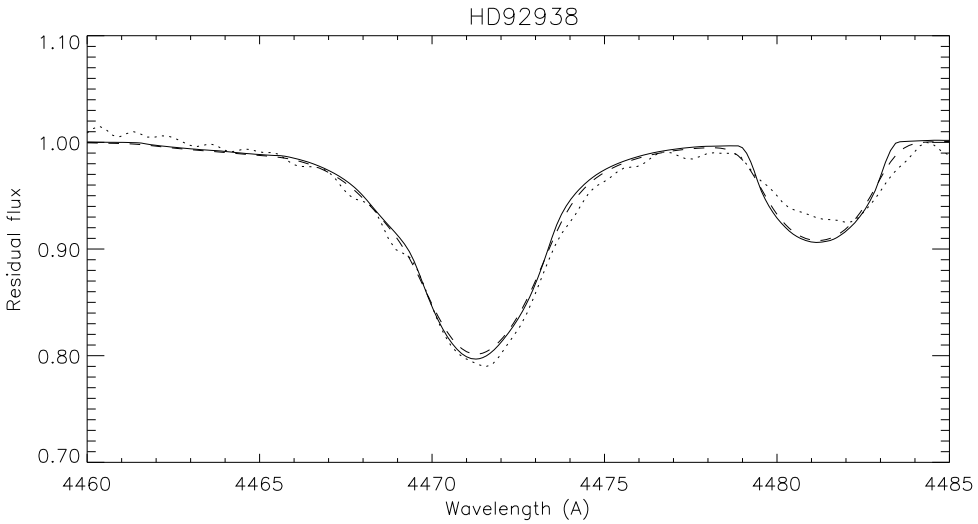

Fig. 6. He I λ 4471 Å line profile of HD 92938, observed coadded spectrum (**dots**) and computed spectrum (**solid** line). Synthetic spectrum computed with a Kurucz (1992) model, convoluted with a rotational profile having $v \sin i$ = 135 kms^{-1} and with a gaussian having FWHM = 1 Å(**dashed** line) which approximates the instrumental profile. The helium abundance was set to 0.19 while a solar abundance was assumed for magnesium; v_{turb}=6 kms^{-1} was adopted.

Table 5 gives the quantitative NLTE effects on the equivalent widths, as well as the effect of the microturbulence. A set of three models was computed, with log g = 4.0 and T_{eff} = 15000 K, 20000 K and 30000 K. We adopted a helium abundance of 0.25. Two microturbulent velocities were considered, namely 1 and 10 kms^{-1} but we assumed that no macroscopic motions take place. The table gives the relative change in percent of the equivalent width. The equivalent width increases when the NLTE effects are taken into account and when the microturbulence varies from 1 kms^{-1} up to 10 kms^{-1}. The behaviour of the b-factors for the transitions 492.2 nm (states 2^1P-4^1D) and 1083.3 nm (states 2^3S-2^3P) are given in Figs. 7 and 8 for model atmospheres with an effective temperature of 15000 K and 30000 K respectively. The common feature is the decrease of b-factors in the outer atmospheric layers. Since the line tansition 402.6nm is sensitive to NLTE for hotter atmospheres we need to stress that the transition is bound to 2^3P and 5^3D states. For upper level, however, approximate relations (collisional rates and b-f cross sections) are used and therefore we may expect the dependence on input data.

Table 5. NLTE and Microturbulence effects. The figures listed are the relative increase in percents, of the equivalent width of the indicated line, when NLTE effects are taken into account and V_{turb} is increased from 1 to 10 kms^{-1} respectively.

		line wavelength (nm)		
T_{eff}	effect	402.6 nm	447.1 nm	492.2 nm
15000	NLTE	1.2	4.3	7.4
	turb.	0.3	2.6	0.2
20000	NLTE	16.0	4.3	4.6
	turb.	2.3	2.9	0.4
30000	NLTE	29.0	6.7	5.7
	turb.	3.1	4.3	0.8

4. Helium abundance and evolutionary state

A correlation between the He abundance and the surface gravity was suspected by Glagolevskij et al. (1992) and by Zboril et al. (1994), and one purpose of this paper is to confirm it on a larger sample. The results of Table 4 are shown in Fig. 9a and the suspected correlation is not confirmed. The regression lines have been fitted taking into account errors on both axes, the er-

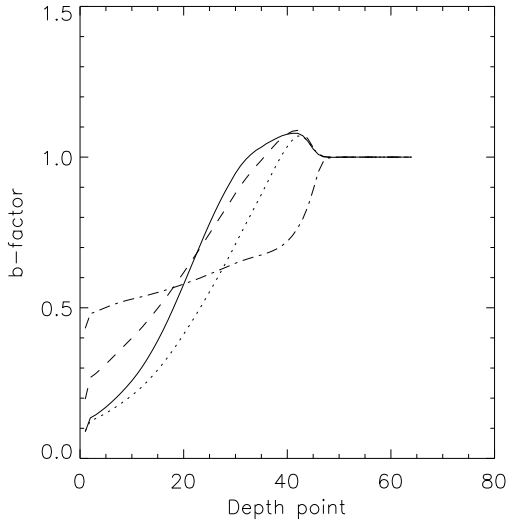

Fig. 7. b-factors of 2^3S (solid line), 2^3P (dotted line), 2^1P (dashed line) and 4^1D (dash dot) neutral helium levels respectively

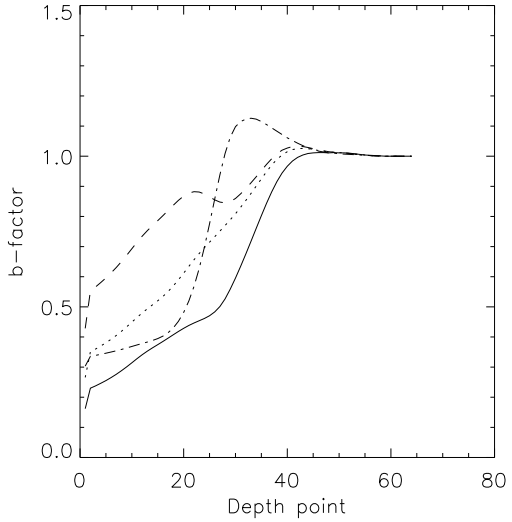

Fig. 8. b-factors of 2^3S (solid line), 2^3P (dotted line), 2^1P (dashed line) and 4^1D (dash dot) neutral helium levels respectively

rors on $n(He)$ being on average three times smaller than those on R/R_z. The statistical significance of the correlation is not great: the Spearman rank correlation coefficients are -0.306 and 0.615 respectively for the black and open dots, corresponding to a Student t test of -1.20 and 2.92, i.e. roughly 70% and 98% probabilities that the correlation is real. The range in R/R_z is rather small for the full dots (the most reliable in principle), which represent the values obtained for the surface gravity by imposing the photometric $T_{\rm eff}$ values, as explained above. We have two extremely He-rich stars, CPD $-62°2124$ and HD 124448 which, however, present emission at least in their Balmer lines so that their helium abundances might be less reliable. HD 124448 being quite atypical of the intermediate He stars, it has been excluded from the above regression. CPD $-62°2124$ was also excluded. On the other hand, several other stars show some emission too but estimates of atmospheric parameters from Geneva photometry and hydrogen profiles are quite consistent. Helium abundances of normal reference stars are quite typical of the abundances in normal stars.

Our data do not allow us to tell definitely whether the "He-rich" phenomenon is uniformly distributed on the whole main sequence width, or not. If we rely entirely on the fits of the Balmer line profiles, then it seems the first term of the alternative holds true, especially if we remember that the log g values are systematically too large by about 0.2 dex. If, on the other hand one relies on the photometric data, corrected for the effect of the He overabundance on the photometric $T_{\rm eff}$ determination, then Fig. 9a indicates that He-rich stars are confined in the vicinity of the ZAMS. The latter conclusion depends on wether the synthetic colours computed in Sect. 3.2 are realistic or not.

The relation between He abundance and position of the star in the HR diagram is quite interesting with regard to the theory of radiatively driven winds in B stars (Babel 1995, 1996). According to Fig. 6 of Babel (1996), the He-rich stars have relatively large, homogeneous winds which permit He to be overabundant in their photospheres in spite of the small radiative acceleration. Since the wind is larger when the luminosity is larger, one can qualitatively expect the He abundance to be larger as well, so a correlation between n(He) and $\log L/L_\odot$ has been looked for (the luminosity has been obtained from the *ages.f* code kindly provided by F. Figueras and C. Jordi, which interpolates theoretical evolutionary tracks for given $T_{\rm eff}$ and $\log g$): Fig. 9b shows that no such correlation exists. However, if the wind is too large, helium will leave the photosphere and will not be overabundant any more. The apparent lack of He-rich stars with small surface gravities may be significant in this respect, but can only be suggested with our data. The sample is small and the uncertainties on the estimated surface gravities are large, making a clear-cut conclusion difficult.

5. Spectroscopic variability

The catalogue of Renson et al. (1991) gives the period of variability when it is known, with the notation 'S' indicating the presence of spectroscopic variations (i.e. intensity of spectral lines), 'V' indicating radial velocity variations, 'M' magnetic field and 'L' luminosity and/or colour variations. For HD 37479, the database reports VSLM-type variability with a 1.191 days period; for HD 58260 there is S variability with a 1.66 days period; for HD 37776 there is SLMV variability with a 1.539 days period and HD 37017 varies (SLM) with a 0.9012 days period. But, at least in helium line profiles, we were unable to detect any variability in our programme stars.

6. Emission

Some of our programme stars display a kind of emission, preferably in the H_β line profile. This feature was even detected in two reference standard stars and probably indicates the presence of a dense wind. Fig. 10 displays the emission in H_β for all stars where it is clearly present. Synthesized profile for HD

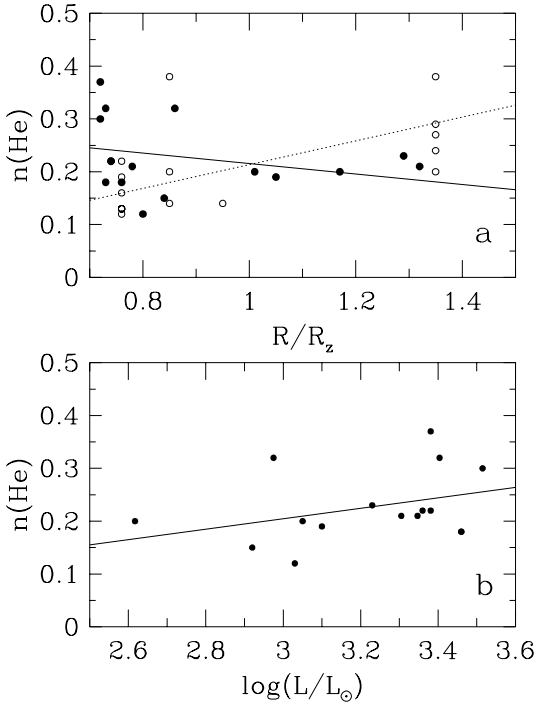

Fig. 9. a Helium abundance versus evolutionary state for the He-rich stars, with purely spectroscopic surface gravities (*open dots*). The *full dots* show the same, but with radii and helium abundances estimated on the basis of photometric values of $T_{\rm eff}$. The solid line has been fitted to the full dots, allowing for errors in both axes. The dotted line is the same for the open dots. **b** Relation between He abundance and luminosity (same symbols as above).

56139 was computed using LTE Kurucz (1992) models with a chromospheric structure which basically follows the expression

$$T(dm) = T_{Kur}(dm) + T_{chrom.}(dm) \quad (7)$$

where dm is the mass depth variable and T the temperature. The chromosphere was added to the photospheric model following roughly the solar model, i.e. for mass depth variable less than 0.01 there is a "chromospheric" temperature rise, followed by a plateau and by another, corona-like rise in temperature. The purpose was not to find the temperature structure in such stars, but rather to give an idea how different the $T(\tau)$ relation maybe in their high atmosphere, compared with those stars showing no emission. The observed profile of HD 56139 indicates agreement in the far line wings, while the line core suggests a different kind of atmospheric structure. There is also a red-shift observed here. Other stars indicate various levels of activity in the atmosphere. In the case of HD 105435 we probably meet saturation and/or dynamical range effect since instrumentation was set up for absorption. Hydrogen line profile of HD 37479 demonstrates that a kind of emission is recognized in Geneva photometry (from a comparison with the β index observed in $uvby\beta$ photometry) while the line profile is almost regular. A model atmosphere study of these stars with emission will be published elsewhere. We restrict ourselves here only by formulating a statement that hydrogen beta line profile resembles more a Be phenomenon than a $Bshell$ one. Studies of early type stars with emission indicate these phenomena may even occur and disappear in one and the same star and are therefore time dependent: likewise, we are able to detect marginal variability in Hβ in HD37479 at about the 15 percent level, the Be-type emission being always present. Possible variability in the case of HD 124448 is no more than 2 percent, if any. For other stars with emission in Hβ we have unfortunately single records. The star CPD $-62°2124$ deserves a special comment, since the Balmer lines are seen in emission not only in the star but also in the surrounding sky. Therefore the origin of the emission lies in a nebula which not necessarily surrounds the star but may be in the foreground or in the background; there is no reason to believe that the emission is taking place in any circumstellar material.

7. Conclusions

The abundance analysis of 24 (19 He-r and 5 standard) stars was carried out using spectrum synthesis computations to evaluate primarily helium abundance and its possible link with the evolutionary state, which was suspected in previous papers. Helium abundances were obtained using current Kurucz models. The trend found in our previous papers, i.e. an increase of the helium abundance with decreasing log g or with increasing radius, cannot be confirmed. If such a trend existed at all, it would be extremely loose in any case. The radius was obtained from the surface gravity through the formula $R \sim 1/\sqrt{g}$. Since we could use three hydrogen line profiles, we could determine the surface gravities with a better reliability. However, an unexpected problem arose in the scale of the effective temperatures, which is 1300 K larger for photometric than for spectroscopic estimates. Taking into account the effect of the helium overabundance on the Geneva colours as well as on the computed Balmer line profiles resolves this discrepancy. The method we have used here for determining the radius of the star relative to its ZAMS value is more precise than that used in our previous papers, where we relied on the definition of the luminosity of a star: $L=4\pi R^2\sigma T^4$ resulting in the following expression for the radius

$$log\ R = 8.46 - 2log\ T_{eff} - 0.2M_{bol} \quad (8)$$

if corresponding solar quantities are taken account. However, to obtain the bolometric magnitude, we relied on the β index, which may be quite peculiar for many He-rich stars (emission in H_β). Furthermore, the He-rich stars lie on the boundary of the $c1 - H\beta$ relation, where the calibration $\beta \sim M_v(\beta)$ may not be valid. Besides, another calibration step has to be done to obtain the effective temperature and bolometric magnitude. Finally, any error on M_{bol} enters linearly into the above formula.

The direct comparison with previous reports on the evolutionary state of the He-rich stars (Zboril et al. 1994) is not easy. The atmospheric parameters estimates were based on pure photometric methods and Geneva photometry was only one of them. Thus both R/R_z and helium abundances may have been blurred. We also used the relation given above. Several stars observed here were analysed in our previous paper but they

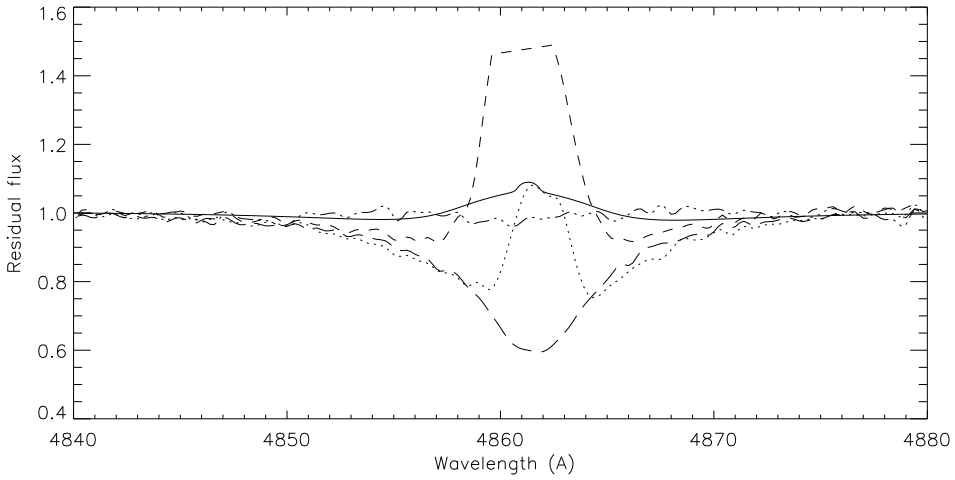

Fig. 10. H_β line profile for stars in Table 4. **Solid line:** synthesized profile from a model atmosphere with "chromosphere" and "corona", and a photospheric structure corresponding to an LTE Kurucz model atmosphere (1992) of the star HD 56139. **dotted line:** observed profile for the standard star HD 56139. **dashed line:** observed profile for HD 105435. **dash dot dot dot:** observed profile for HD124448. **long dash:** observed profile for HD 37479. See text.

cover here a narrower R/R$_z$ interval. This trend holds for all programme stars. The helium abundance interval, however, corresponds very well with the previous paper. Only very active stars in this paper possess very high helium abundance ($\sim$ 0.6-0.8) based on Kurucz models. Synthesized Geneva colours for non-solar He abundances show a systematic trend, especially for the $[U-B]$ index which decreases by about 0.025 mag per 0.1 He abundance. The effect decreases with increasing effective temperature. This in turn leads to an overestimate of the effective temperature if standard photometric calibrations (based on solar-abundance Kurucz models) are used. We can expect also the hydrogen line profiles may be affected. They depend non-linearly on the three quantities $T_{\rm eff}$, $\log g$, $n(He)$ and since we do not know apriori $n(He)$, this fact may explain a systematic shift compared with theoretical evolutionary tracks.

Comparing our equivalent width measurements with Walborn's, we found considerable discrepancies, which may reach up to 40%. The S/N of Walborn's spectra is in the range 10-20. Modelling hydrogen profiles and adding this S/N to the theoretical profiles we met the following effect: the equivalent width is increased due to low S/N and increasing interval for locating the continuum level in such noisy data. This alone leads to a 30-40% increase of the equivalent width. If we add the scaling problem Walborn met, it is possible to explain the difference between our measurements and Walborn's, at least in the case of hydrogen profiles shown in figure 1. As helium lines have a smaller equivalent width, one may also expect a larger scatter (in relative value) for a given S/N.

Acknowledgements. MZ wishes to acknowledge gratefully an UK PPARC grant support. PN thanks Dr. Gautier Mathys and the night assistants at ESO La Silla for their help, and the Swiss National Science Foundation for its support. Some photometric measurements made in the Geneva system at La Silla by Dr. Michel Burnet are also gratefully acknowledged.

References

Babel J. 1995, A&A 301, 823
Babel J. 1996, A&A 309, 867
Barnard A.J, Cooper J., Smith E.W., 1974, J. Quant. Spectrosc. Radiat. Transfer 14, 1025
Bohlender D.A., Landstreet J.D., Brown D.N., Thompson I.B., 1987, ApJ 323, 325
Cramer, N., Maeder, A., 1979, A&A 78, 305
Dimitrijevic M. S., Sahal-Brechot S. 1984, J. Quant. Spectrosc. Radiat. Transfer., 31, 301
Glagolevskij Yu. V. 1990, in"Hot chemically peculiar and magnetic stars", Proceedings of 8th subcommission "Magnetic stars", eds. G. Scholz, Potsdam-Babelsberg, Germany, p.62
Glagolevskij Yu. V., Topilskaya G. P., Kartashova T. A. 1992, in "Stellar Magnetism", eds. Yu. V. Glagolevskij and I. I. Romanyuk, Russian Academy of Sciences, "NAUKA", Sankt-Petersburg, p.62
Hubeny I., Lanz T. 1992, A&A, 262, 171
Kilian J. 1992, A&A, 262, 501
Kurucz R.L. 1992, Rev. Mex. Astron. Astrofis. 23,45
Kűnzli, M., North P., Kurucz, R.L, Nicolet, B., 1997, A&AS, 122, 51
Michaud G., Dupuis J., Fontaine G., Montmerle T., 1987, ApJ 322, 302
Mihalas D., Heasley J. N.A, Auer L. H. 1975, NCAR-TN/STR-104
North, P. and Paltani, S. 1994, A&AS, 288, 155
Pedersen H., 1979, A&AS 35, 313
Pedersen H., Thomsen B., 1977, A&AS 30, 11
Prinja R.K., Barlow M.J., Howarth I.D. 1990, ApJ, 361, 607
Renson P., Gerbaldi M., Catalano F.A., 1991, A&AS, 89, 429
Rufener F., Nicolet B., 1988, A&A 206, 357
Shamey P., 1969, PhD thesis, unpublished
Schaller G., Schaerer D., Meynet G., Maeder A., 1992, A&AS, 96, 269
Schild R., Peterson D. M., Oke J. B., 1971, ApJ 166,95
Schoening T., Butler K. 1989, *Astron. Astrophys. Suppl. Ser.*, 78,51
Schönberner, D., Wolf, R.E.A., 1974, A&A 37, 87
Slettebak A., Collins II G.W., Boyce P.B., White N.M., Parkinson T.P., 1975, AJS 29, 137
Vauclair S., 1975, A&A 45, 233
Vauclair S., Dolez, N., Gough, D.O., 1991, A&A 252, 618
Walborn N.R., 1983, ApJ 268, 195
Zboril M., Glagolevskij Yu. V., North P. 1994, in "International Conference on CP and Magnetic Stars", Tatranská Lomnica, eds. J. Zverko and J. Žižňovský, p. 105
Zboril M., 1996, in: Model Atmospheres and Spectrum Synthesis, eds. S.J. Adelman, F. Kupka, and W.W. Weiss, ASP Conf. Series Vol. 108, p. 193

This article was processed by the author using Springer-Verlag LaTeX A&A style file *L-AA* version 3.